

The refurbishing of used salt water reverse osmosis composite membranes

Orli Weizman^a, Eran Peri^a, Lev Masturov^a, Ofer Chertkoff^a, Iris Sutzkover-Gutman^b, Avner Hermoni^b, Dan Y. Lewitus^{a,*}

^aThe Pernick Faculty of Engineering Department of Polymers and Plastics Engineering, Shenkar College, Ramat-Gan, Israel, Tel. +97236130111; email: lewitus@shenkar.ac.il (D.Y. Lewitus), Tel. +97236130111; emails: orli1910@shenkar.ac.il (O. Weizman), eranperi1@gmail.com (E. Peri), levi.masturov@gmail.com (L. Masturov), oferiko170@gmail.com (O. Chertkoff)

^bVia Maris Operation Ltd., Palmachim SWRO Desalination Plant, Israel, emails: avnerh@vmd.co.il (A. Hermoni), iris@vmd.co.il (I. Sutzkover-Gutman)

Received 2 September 2019; Accepted 5 February 2020

ABSTRACT

This work presents the potential to repair used and dysfunctional reverse osmosis (RO) composite membranes. Under constant use, polyamide-based RO membranes exhibit a timely deterioration in salt rejection and water permeability from the values purported by their manufacturer. Manufacturers typically anticipate a 5%–7% decline of both characteristics. These changes are caused by an accumulation of various phenomena, including membrane matrix aging, fouling, and mechanical or chemical deterioration. The present work aims to allow the reuse of damaged RO membranes, which present a reduction in salt rejection together with an increase in flux, due to the deterioration of the polyamide barrier layer on their upper surface. Deficient membranes taken from desalination plants were cleaned, followed by the repair of the thermoset polyamide layer via interfacial repolymerization with trimesoyl chloride through a simple refurbishing process. Membranes were tested using a laboratory-scale crossflow RO test unit. It was found that while plant-used, defect membrane, exhibited a poor performance (salt rejection of 81% with a flux of 83 L/m²/h), once repaired, the membranes exhibited a substantial increase in salt rejection capacity (95%) and reduction in flux (36 L/m²/h). These results were in par with virgin membranes (salt rejection of 95% and flux of 42 L/m²/h). The repolymerization refurbishing technique and its resulting membrane physiochemical characteristics are described in detail.

Keywords: Desalination; Reverse osmosis membranes; Repolymerization; Refurbish

1. Introduction

10.5 billion gallons per day is the expected desalination capacity in the world in 20 y, practically doubling today's capacity. About two-thirds of these desalinate seawater in designated plants [1]. Reverse osmosis (RO) technology was developed over 50 y ago and has become the fastest-growing segment of the seawater desalination market, with currently a total of 9,000 plants worldwide [2]. Although the RO process is considered a successful technique for seawater

desalination, it is still requiring several times more energy-intensive over traditional treatments of a freshwater resource. (specific energy consumption of 3.5–4.5 kWh/m³ for a real-scale seawater reverse osmosis (SWRO) process vs. 0.2–0.4 kWh/m³ for conventional treatments of surface water) [3]. Consequently, new technological improvements to reduce desalinate water production energy are frequently appeared [4]. The steady trend of reduction of SWRO energy requirements and costs together with increasing costs of conventional water treatment and water reuse due to more

* Corresponding author.

stringent regulatory requirements are expected to accelerate the SWRO market and the preference of the ocean as the water source.

RO is a process based on a pressure-driven membrane, where a polymer membrane is in the heart of the process, separating the unwanted ions from a feed to obtain the desired low-salinity product. The separation characteristics and the membrane properties mostly depend on the chemical and mechanical structure of the membrane materials.

Thin-film composite (TFC) polyamide membranes dominate the market of RO membranes. To prepare the TFC membrane, interfacial polymerization (IP) techniques are mostly used resulting in three-layer structure: A structural support layer (120–150 μm thick) made of the polyester web which provides mechanical support to the active layer; a microporous polysulfone interlayer (50 μm thick) that can withstand high-pressure compression; and an ultra-thin polyamide barrier layer on the upper surface (about 0.1 μm in thickness). This layer is the active layer that controls membrane performance (permeability and selectivity). To achieve high values of permeability and selectivity, the active layer should have an ultrathin thickness and a hydrophilic nature [5]. TFC RO membranes achieve salt rejection level consistently higher than 99%, at its standard test conditions, the seawater element has a typical value of 99.8% while the brackish water element has a typical value of 99.5% [6]. The ultra-thin polyamide films synthesized via IP can display a range of physical and chemical properties, based on the polymerization conditions including the monomers concentrations and the reactant ratios [7–12].

The fast-growing use of RO membranes in the sea and brackish water purification is mainly attributed to the development of more sustainable membrane technologies that have lowered the cost of membrane modules and produced a higher quality filtrate [4]. Still, the process of RO desalination suffers from serious concerns. A major problem is the accumulation of organic and inorganic fouling on the membrane surface that negatively affects its performance due to the chemical degradation of the active membrane layer [7]. Fouling causes a serious decline in flux and filtrate quality and ultimately causes an increase in the operating pressure with time [8,9]. The major efforts of the membrane research and the desalination industries have been to enhance, or at least maintain, water flux, and salt rejection for longer periods, thus increase efficiency and reduce operating costs. To maintain the high desalination capacities fouling problem requires frequent chemical cleaning that ultimately shortens membrane life through damage to the barrier layer, thus imposing a large economic concern on RO membrane plant operation [10]. In addition to the fouling accumulation problem, according to desalination plants, membrane replacement is also required due to the timely decline of salt rejection capacity, resulting from the pressure gradient in operating RO membranes. This mechanical model of failure limits the membranes life-cycle due to breaching of the ultra-thin polyamide layer which associated with the formation of ridges/cracks and chemical degradation on the PA layer.

So far, used RO modules are considered as common waste, with quantities that dramatically increase around the world as the use in RO become more popular. Used-damaged

membranes are commonly buried in municipal landfills, with few disposal alternatives proposed to RO users. The environmental impact of this non-biodegradable membrane waste is remarkable, as the annum volume of a single seawater RO plant is in the range of 100–200 m^3 . This major drawback led to increased researchers interested in the reuse options of wasted RO membrane [6,7,10]. Alternatively, the modification and development of higher performance RO membrane are undertaken, including improvements in membrane materials, module and process design, and energy recovery [6,11–19].

To date, no evidence exists of efforts that are aimed toward the extension of a RO membrane life through refurbishing of old used and worn out membranes towards reuse in seawater RO technology. This effort will be undertaken in the present work by *in-situ* interfacial repolymerization reaction of the ultra-thin polyamide (PA) layer using one or two of the monomers, MPD in water and TMC in hexane. This technique proposes to step forward in the approach toward the refurbishing of the active layer, potentially allowing recovered performances of the damaged membrane, including rejection ability and an increase of flux at least for the same level as in a virgin membrane, which will allow their reuse in desalination plants.

2. Experimental

2.1. Materials

RO membranes [Filmtec SW-XLE440, Dow Water and Process Solutions (Edina, MN)] were kindly supplied by Via Maris Desalination Ltd. (Palmachim, IL). Virgin, control membranes were used as received. Used membranes were such that served at the Via Maris plant for at least 2 y, and were identified by the operators as dysfunctional membranes due to their poor desalination performance. The reactive monomers and solvents used in this work were *m*-phenylenediamine (MPD, $\geq 99\%$) and trimesoyl chloride (TMC, 98%), Deionized (DI) water, and *n*-hexane (anhydrous $\geq 95\%$). All chemicals were purchased from Sigma-Aldrich (St. Louis, MO).

2.2. Preparation method

To allow the simple application of the PA monomers onto the existing damaged polyamide layer, a dipping-based IP protocol was used. The selection of the reactive monomers solution concentrations for the refurbishing process was based on existing polyamide-based RO membranes preparation protocols [20–22].

Flat sheet membranes samples (138 cm^2) were cut from the supplied TFC membranes and were immersed in DI water for about one hour to remove accumulated dirt and residue salts. The washed membranes were then placed in a plastic container filled with MPD aqueous solution at 2 wt.% at RT. After a 10 s immersion, membranes were removed from the container and let dry in a chemical hood to remove excess MPD solution. Membranes were then immersed for 10 s in a plastic container filled with TMC in Hexane at 0.1 wt.% at RT. After immersion, membranes were removed, washed by hexane and dried in a chemical hood. Finally, the prepared

refurbished membranes were immersed in DI water until further use. To allow better insight into the chemical processes occurring during the refurbishing process, a variation on the aforementioned process was applied. In the first, only TMC monomer was used, and in the second TMC + MPD was applied. This was performed to evaluate whether the monomers can react with the residual functional groups exposed on the damaged reactive PA thin layer surface during its lifetime use [23]. Virgin and used commercial RO membranes were used as reference samples for performance comparison. The prepared refurbished membranes formulations are detailed in Table 1.

2.3. Testing and characterization

The performance of the membranes was examined in terms of salt rejection efficiency and water flux carried out using a lab-scale membrane flat sheet test rig. The observed results were correlated to changes in the chemical and morphological properties of the PA layer, carried out by scanning electron microscopy (SEM), X-ray photoelectron spectroscopy (XPS), Fourier transform infrared spectroscopy (FTIR), atomic force microscopy (AFM), and contact angle (CA) measurement.

2.3.1. Membrane flat sheet test rig

Membrane flat sheet test rig (SEPA CF Cell STERLITECH Corporation, Kent, WA 98032-1911 USA) with a lab-scale crossflow filtration was used to provide fast and accurate performance data of the desalination capabilities of given RO membranes in terms of flux and salt rejection. However, it should be noted that the applied pressure in our membrane element cell was limited to 40 bar, thus the performance of given RO membrane sample was expected to be lower than that of membranes operate in standard desalination plants under much higher pressure conditions of ~60–70 bar (68 bar) [24]. Yet, the flat sheet membrane cell is believed to have the ability to provide us comparative values in a real-time simulation of the larger, industrial spiral wound membranes.

The flat sheet membrane cell was operated as follows: A flat sheet membrane with an area of 138 cm² was sealed in the cell body. An O-ring was placed in the cell body to prevent leaking and generate an effective area. Hydraulic pressure of 1,200 bar was applied, to compress the cell body against the cell holder top to make sure that there will be no leaking from the cell. The feed stream was pumped at a trans-membrane pressure of 40 bar, from the feed tank to the feed inlet and the feed flow was forced into the membrane cavity. The total volume of the feed tank was 5 L. The feed tank was equipped with a temperature control system maintained at

23°C ± 3°C. In the cavity, the feed flows tangentially across the membrane. A portion of feed flows through the permeate carrier to the center of the cell body top and then flows through the permeate outlet into a collection vessel. The performance and efficiency of the desalination process for the different membranes were measured and calculated according to the equations listed below. Measurement was repeated on three different samples for each membrane module. The mean results and standard deviations are reported.

The flow rate was carried out by measuring the time required to fill 20 mL of desalinated water into a collection vessel. The value of permeation flux (J_p) was calculated using Eq. (1).

$$J_p \left(\text{Lm}^{-2}\text{h}^{-1} \right) = \frac{\text{Flow} \left(\text{Ls}^{-1} \right) \times 3,600 \left(\text{s/h} \right)}{\text{membrane area} \left(\text{m}^2 \right)} \quad (1)$$

Additionally, the salt rejection level of the membranes was characterized. The concentration of the salt in the feed and permeate solutions was determined by measurements of electrical conductivity. Feed solution salinity was kept constant at 3,750 ppm of sodium chloride in distilled water (by setting the solution conductivity to 7.5 mS/cm).

$$R(\%) = \frac{C_f - C_p}{C_f} \times 100 \quad (2)$$

where R is defined as the fraction of solute retained by the membrane for a given concentration of feed solution. C_f is the sodium chloride concentration in the feed and C_p is the concentration in the permeate.

2.3.2. Contact angle

CA measurement was carried out on the PA layer of the membrane using the sessile drop method with a “Data Physics” OCA 20 contact angle measurement apparatus by ASTM D7334. CA provided insight into the surface hydrophobicity of the membrane’s upper surface and its underlying chemistry. A standard deionized, ultra-filtered water droplet volume of 5 μL was set for all static contact angle measurements. Contact angle (θ) was recorded live using a computer connected CCD camera equipped with an X10 magnification lens located on the apparatus. Snapshots were taken after 10 s of droplet contact with the surface. Contact angle measurement was performed with computer-assisted graphical tools (SCA 20 software). The mean θ value for the surface of each sample and the standard deviation was calculated from five measurements.

Table 1
PA layer polymerization synthesis formulation of refurbished membranes

Refurbished membranes samples	PA repolymerization synthesis formulation	
	MPD conc. (wt.%) in aqueous solution	TMC conc. (wt.%) in hexane solution
TMC	0	0.1
MPD + TMC	2	0.1

2.3.3. X-ray photoelectron spectroscopy

X-ray photoelectron spectrometer (ESCALAB 250) ultrahigh vacuum (1×10^{-9} bar) apparatus with an Al K-alpha radiation X-ray source and a monochromator was used to obtain the elemental composition at the top PA thin active layer. The X-ray beam size was 500 μm . The survey spectra were recorded with pass energy (PE) of 150 eV and the high energy resolution spectra were recorded with PE of 20 eV. Charging effects were corrected by calibration to a relative carbon C 1s peak positioned at 284.8 eV. Analysis of the XPS results was carried out using AVANTGE program.

2.3.4. Attenuated total reflectance–Fourier-transform infrared spectroscopy

Membrane's surface IR spectra were performed using a Bruker Alpha-P ATR-IR. Spectra were recorded in a range of 400–4,000 cm^{-1} at a resolution of 2 cm^{-1} with 24 scans.

2.3.5. Atomic force microscopy

AFM was used to provide topographic images and phase images of the scanned membranes per ASTM E2382. Polyamide surface morphology of the RO membranes was analyzed using an Innova AFM mounted on an active anti-vibration table with a "Bruker" non-contact silicon probe (Micro-fabricated Si oxide RTESP Ultrasharp with integrated pyramidal tips). The 512 \times 512-pixel images were taken in tapping mode with a scan size of up to 10 μm at a scan rate of 0.5 Hz. Also, the average roughness (Ra) was calculated using the data from the images with "NanoScope Analysis" (Bruker, Billerica, Mahusetts, USA; version 1.40) software. Four different images were taken of each sample.

2.3.6. Scanning electron microscopy

Membrane surface morphology analysis was carried out using high-resolution scanning electron microscopy (HR-SEM, Zeiss Gemini Ultra plus). The applied accelerating voltage was 10 keV.

3. Results and discussion

3.1. Desalination performance

Water permeate flux and salt rejection level of the refurbished and reference membranes were evaluated by the crossflow filtration unit. Fig. 1 presents the performance of the membranes. The results show that the virgin membranes have a higher salt rejection level (about 14% higher) and a lower flux (one-half) compared to the used membranes. These results are attributed to a failure in the PA surface layer, enabling salt impurities to permeate through the membrane resulting in a decrease in salt rejection values while allowing an increase of water flux. However, when treated with each one of the tested procedures, used membranes performance reached, or even exceeded those of a virgin membrane. As expected, the flux values of the treated membranes significantly reduced in comparison to the used membrane. However, while TMC + MPD treated membranes showed lower flux than the virgin membrane, the flux value of the treated membrane with TMC only was similar to that of a virgin membrane. These results can indicate features changes appear in the PA top layer of the used membranes after the different refurbishing process. The low flux results of the TMC + MPD treated membrane (13.9 $\text{L}/\text{m}^2/\text{h}$) compared to the virgin (42.1 $\text{L}/\text{m}^2/\text{h}$) or TMC treated (35.8 $\text{L}/\text{m}^2/\text{h}$) membranes could be attributed to the use of both monomers solutions for the chemical repolymerization of the PA surface layer in the case of the TMC + MPD treatment. Using both monomers can lead to the formation of a too dense and thick PA new layer, which might affect directly on the water flux and salt rejection capabilities of the treated membranes. Based on these results, TMC + MPD treatment seems to have no benefit in comparison with TMC treatment only. Thus, the next characterization parts displayed only the results of the TMC treated membrane in comparison to the reference membranes.

3.2. Hydrophobicity

Contact angle measurements were utilized as an indication of the hydrophobicity of the PA active surface of the RO membrane. Fig. 2 show the differences in the contact

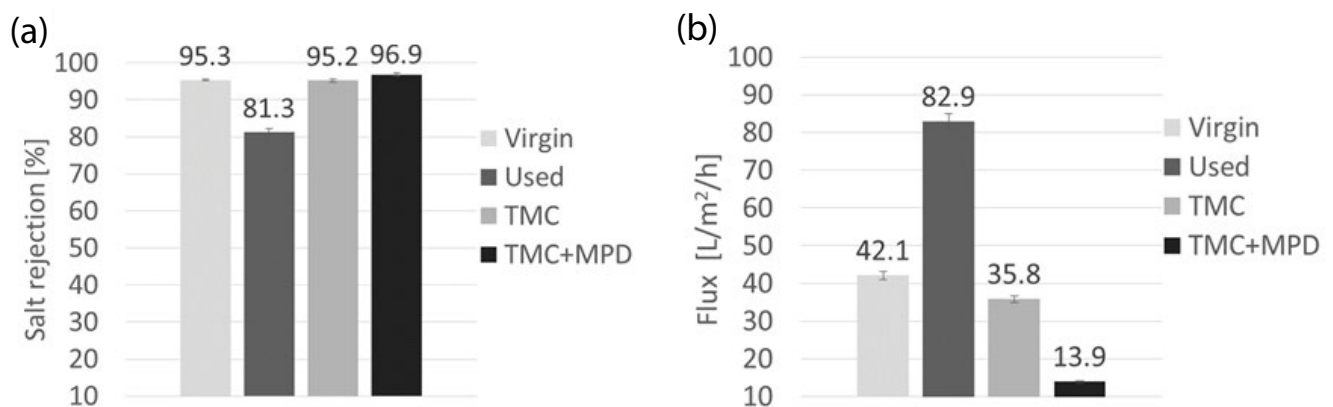


Fig. 1. Salt rejection (a) and Permeation flux (b) of four types of membranes (virgin, used, used treated with TMC, and used treated with TMC + MPD) as measured using membrane element cell under an applied pressure of 40 bar.

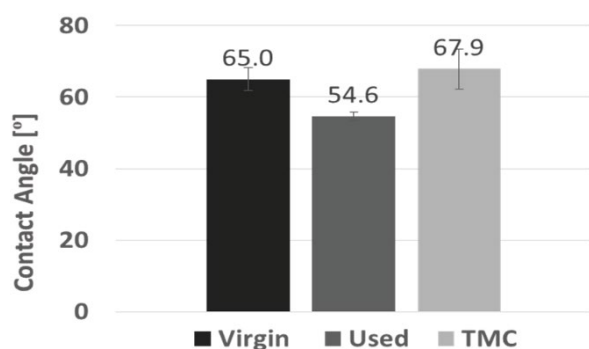


Fig. 2. Water contact angle results for virgin membranes, used membranes, and used membrane after treating with TMC (refurbished).

angle measurements of used membranes before and after interfacial repolymerization, compared to a virgin membrane. Based on known interpretations of contact angle measurements, all membranes tested were hydrophilic (contact angles between 0° and 90°). The contact angle of the used membrane (54.6°) was lower than that of the virgin membrane, indicating a possible surface chemical change, and an increased in surface tension. Once TMC treated was applied, the higher contact angle (67.9°) indicates that the repolymerization process may increase the surface hydrophobicity of the membrane and thus decreased the surface energy close to that of the virgin membrane. Although similar results of contact angle were observed for the treated and virgin membranes, poor correlation of hydrophobicity with membrane fouling or flux properties were found in the literature [25,26]. Thus, it is difficult to use these results to support the membrane performances shown previously and it is suggested to conduct further studies on the issue.

3.3. Surface chemistry

3.3.1. XPS analysis

To show the successful interfacial repolymerization of the PA layer in the TMC treated membrane XPS analyses were performed. The chemical structure of the polyamide active layer was determined using the X-ray photoelectron spectroscope. Since the RO membrane is a composite membrane consisting of a polyamide layer on a Polysulfone support layer, the XPS depth profile was fixed to 10 nm to analyze the near-surface region of the PA film alone without the Polysulfone. The elements studied were C, N, and O, which are elemental characteristics of the polyamide in addition to S element which is elemental of Polysulfone that might appear in the case of a failure in the integrity of the

PA active layer. The C 1s, N 1s, O 1s, and S 2p quantification resulting from the XPS spectra of the membranes are illustrated in Table 2. It can be observed that the used membranes contain S elements while a virgin and TMC treated membrane showed no or negligible quantities of sulfur. The absence of S on the surface of the membranes indicating that the membranes are integrally skinned. This means that the repolymerization protocol successfully restored most of the polyamide matrix. In addition, the typical atomic concentration of aromatic polyamide C, O, and N, can help us to explain the different behavior on the desalination process. TMC treatment on the used membrane has resulted in a higher concentration of nitrogen on the PA surface layer reaching to similar nitrogen amount of a Virgin membrane. Furthermore, an increase in the carbon concentration was observed while the oxygen amount was decreased. Several studies have used the XPS analysis to evaluate the degree of cross-linking of the PA layer [7], based on the O/N ratio. However, in the current study, this calculation could not be performed as the oxygen concentration on the PA surface layer was too high for all types of membranes. Yet, the O/N ratio of a used membrane after treating with TMC was more comparable to that of the virgin membrane, possibly indicating that their theoretical degree of crosslinking was similar.

3.3.2. Attenuated total reflectance–Fourier-transform infrared spectroscopy analysis

Fig. 3 illustrates the ATR-FTIR spectra of a used and a TMC refurbished membrane. N–H bend near $15,580\text{ cm}^{-1}$, the C=C ring vibrations near $1,680\text{ cm}^{-1}$, were visible in both membranes [27]. Yet, both the N–H bend and the C=C ring vibrations increases in intensity in the refurbished membrane, with the former being closer to that of a virgin membrane, while the latter being more prominent than both the used, and the virgin membranes. These data corroborate with the XPS data, where nitrogen is present, possibly in its primary or secondary forms, in the used membrane, and available for reaction with TMC. The observed increase in both nitrogen (from amines), and carbon (from aromatic rings) in the refurbished membrane, probably result from the repolymerization process. Surface polymerization is a complex phenomenon, and one could expect the formation of a polymer, that includes both TMC and MPC residues, and not just TMC-originated carbon.

3.4. Surface morphology and roughness

Characterization of the surface morphological structure is of primary importance for the essential understanding of the membrane performance. Fig. 4 revealed the surface

Table 2
Elemental atomic concentrations of the membranes

Membranes samples	%O	%N	%C	%S	O/N ratio
Virgin membrane	44.13	5.02	40.27	0.00	8.79
Used membrane	45.70	3.25	34.98	0.50	14.06
TMC treated membrane	39.46	5.07	45.40	0.02	7.78

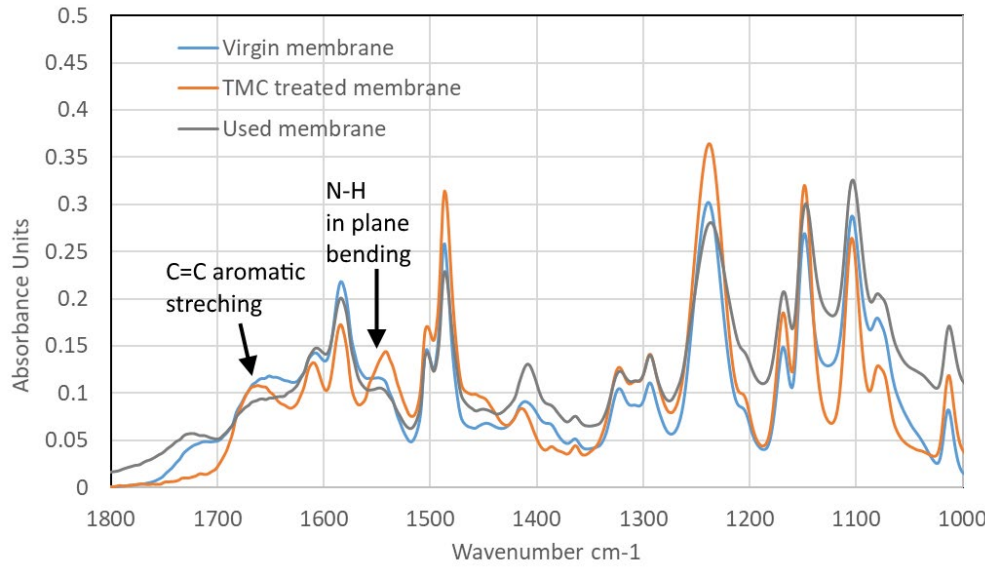


Fig. 3. ATR-FTIR spectra of virgin, used, and refurbished membranes.

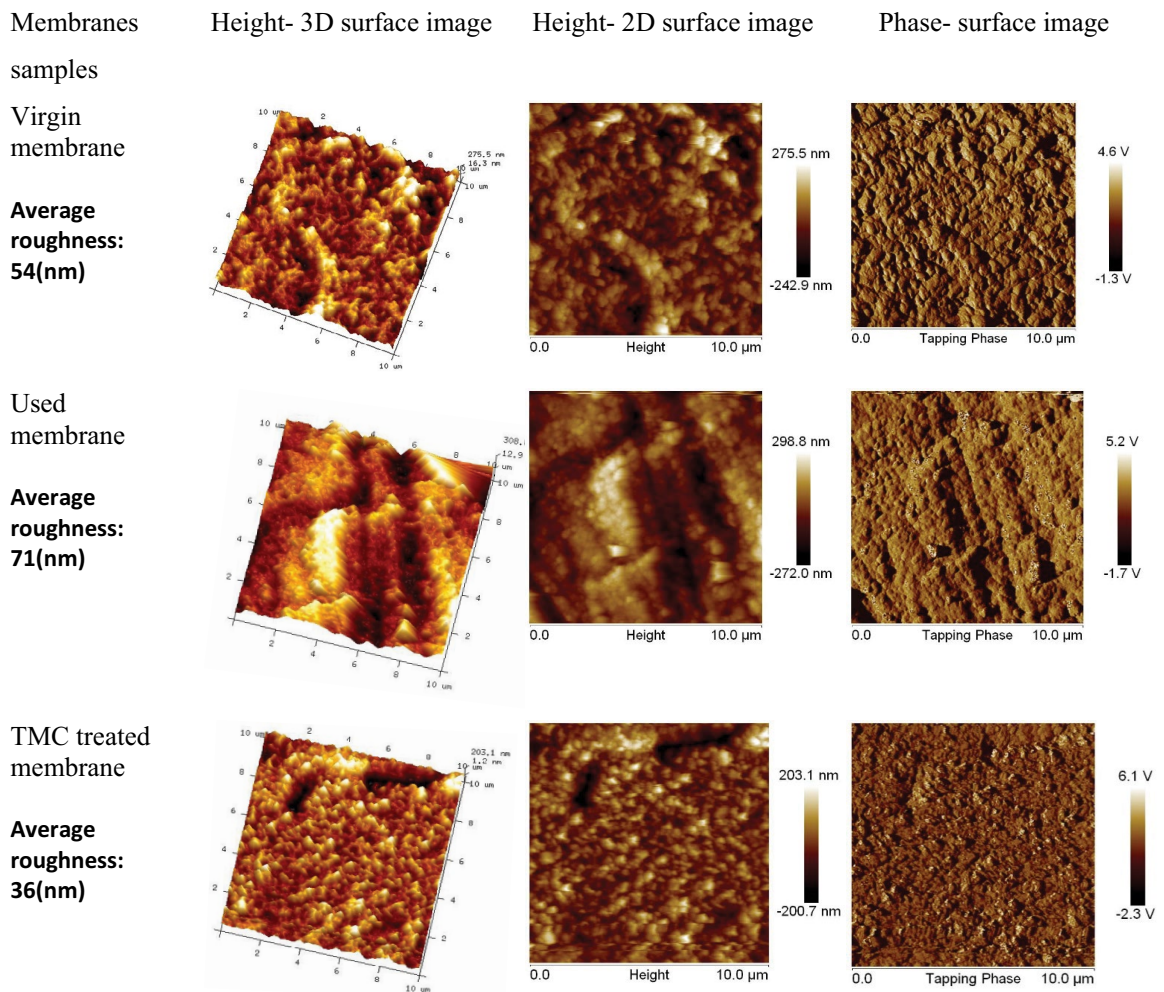


Fig. 4. AFM topography and phase scans for virgin old and TMC treated membranes.

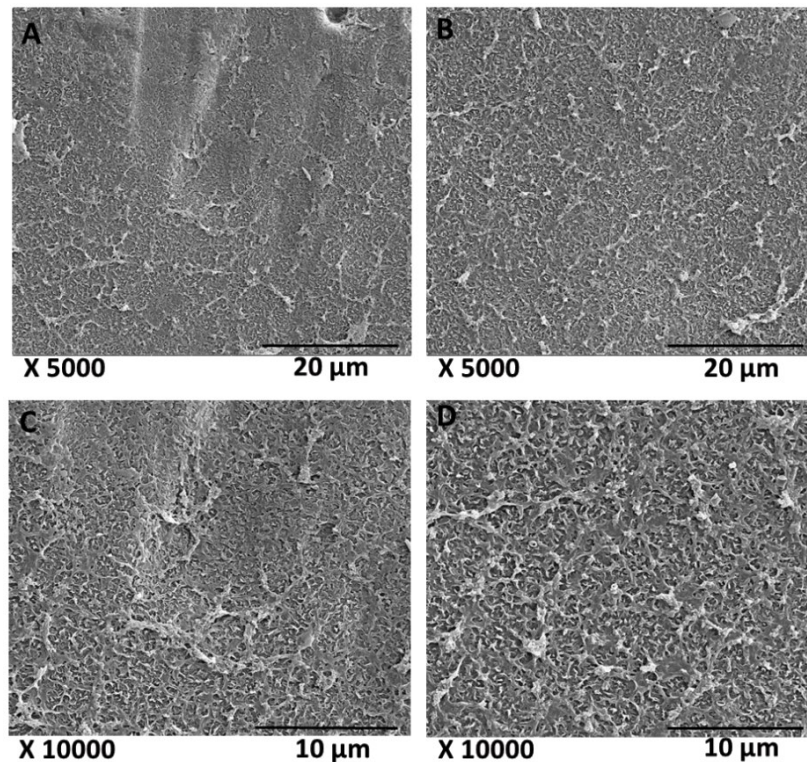


Fig. 5. SEM micrographs of a used membrane (a and c) and a TMC treated membrane (b and d).

morphology of the TMC treated membrane in comparison to the virgin and used membranes. AFM scans of height in 3D and 2D in addition to phase structure and average roughness values are displayed. No evidence of accumulated dirt or residues minerals were distinguished on top of the PA layer of all membrane samples. The surface structure of a typical virgin RO membrane was notable, with the polyamide surface layer's structure covered with "mountainous" peaks. A virgin membrane revealed an average surface roughness of 54 nm. AFM scans of used membranes show a relatively rougher surface (surface roughness of 71 nm) with depressions separated by protrusions. The depressions might correspond to the surface mechanical failures of the used membrane. The surface structural of TMC treated membranes was similar to that of a virgin membrane and different from the used one. In addition, after the treatment of a used membrane with TMC, the surface roughness was significantly decreased to a value of 36 nm. It appears that the repolymerized PA surface covered with mountainous peaks was greatly homogenous and uniform without any depressions on the surface and highest surface area, possibly indicating densification and recovery of the PA layer. Visual assessment of the SEM images showed similar surface features and was in a good agreement with the AFM scans for the membranes tested (Fig. 5). Again, the surface structure of the PA layer of the TMC treated membranes was much more homogenous and uniform compared to the Used one with a similar PA structure of a typical virgin membrane (not shown) [7]. Finally, AFM and SEM scans support the performances of the different membranes by correlating the surface roughness properties and flux results. It has already

been recognized that surface with a smaller average roughness suffered more flux decline since it had more surface features and thus more surface area [25].

4. Conclusions

This study suggests a simple approach towards the refurbishing of the PA layer in an RO membrane. The salt rejection and the water flux were restored and reached the values of a virgin membrane without significantly sacrificing the flux (salt rejection of 95% with a flux of 83 L/m²/h). These findings demonstrate the potential of the suggested method to be scalable to industrial applications and used in desalination plants, were membranes treated by TMC successfully restore the properties of a functioning virgin membrane.

Acknowledgments

The authors would like to thank Via Maris Operation Ltd. (Palmachim SWRO desalination plant, IL), for the assistance in supplying both the RO membranes and the flat sheet membrane cell. This work was funded by the Israel Innovation Authority grant #53597.

References

- [1] T. Pankratz, IDA Desalination Yearbook, Media Analytics Ltd., Oxford, 2010–2011.
- [2] M. Elimelech, W.A Phillip, The future of seawater desalination: energy, technology, and the environment, *Science*, 333 (2011) 712–717.

- [3] J. Kim, K. Park, D. Ryook, S. Hong, A comprehensive review of energy consumption of seawater reverse osmosis desalination plants, *Appl. Energy*, 254 (2019) 113652.
- [4] N. Voutchkov, Energy use for membrane seawater desalination-current status and trends, *Desalination*, 431 (2018) 2–14.
- [5] A.K. Pabby, S.S.H. Rizvi, A.M.S. Requena, *Handbook of Membrane Separations: Chemical, Pharmaceutical, Food, and Biotechnological Applications*, CRC Press, 2015.
- [6] K.P. Lee, T.C. Arnot, D. Mattia, A review of reverse osmosis membrane materials for desalination-development to date and future potential, *Membr. Sci.*, 370 (2011) 1–22.
- [7] W. Lawler, Z. Bradford-Hartke, M.J. Cran, M.C. Duke, G. Leslie, B.P. Ladewig, P. Le-Clech, Towards new opportunities for reuse, recycling and disposal of used reverse osmosis membranes, *Desalination*, 299 (2012) 103–112.
- [8] F.A. Abd El Aleem, K.A. Al-Sugair, M.I. Alahmad, Biofouling problems in membrane processes for water desalination and reuse in Saudi Arabia, *Int. Biodeterior. Biodegrad.*, 41 (1998) 19–23.
- [9] T. Nguyen, F.A. Roddick, L. Fan, Biofouling of water treatment membranes: a review of the underlying causes, monitoring techniques and control measures, *Membranes (Basel)*, 2 (2012) 804–840.
- [10] E.C. de Paula, M. Amaral, Extending the life-cycle of reverse osmosis membranes: a review, *Waste Manage. Res.*, 35 (2017) 456–470.
- [11] R. Bernstein, S. Belfer, V. Freger, Improving performance of spiral wound RO elements by in situ concentration polarization-enhanced radical graft polymerization, *Membr. Sci.*, 405–406 (2012) 79–84.
- [12] K.Y. Jee, D.H. Shin, Y.T. Lee, Surface modification of polyamide RO membrane for improved fouling resistance, *Desalination*, 394 (2016) 131–137.
- [13] O. Choi, P.G. Ingole, H.-K. Lee, Preparation and characterization of thin film composite membrane for the removal of water vapor from the flue gas at bench scale, *Sep. Purif. Technol.*, 211 (2019) 401–407.
- [14] P.G. Ingole, W.K. Choi, G.B. Lee, H.K. Lee, Thin-film-composite hollow-fiber membranes for water vapor separation, *Desalination*, 403 (2017) 12–23.
- [15] T. Fujioka, L.D. Nghiem, Modification of a polyamide reverse osmosis membrane by heat treatment for enhanced fouling resistance, *Water Sci. Technol. Water Supply*, 13 (2013) 1553–1559.
- [16] S. Inukai, R. Cruz-Silva, J. Ortiz-Medina, A. Morelos-Gomez, K. Takeuchi, T. Hayashi, A. Tanioka, T. Araki, S. Tejima, T. Noguchi, M. Terrones, M. Endo, High-performance multi-functional reverse osmosis membranes obtained by carbon nanotube-polyamide nanocomposite, *Sci. Rep.*, 5 (2015) 13562.
- [17] J. Kim, S. Hong, A novel single-pass reverse osmosis configuration for high-purity water production and low energy consumption in seawater desalination, *Desalination*, 429 (2018) 142–154.
- [18] J. Kim, S. Hong, Optimizing seawater reverse osmosis with internally staged design to improve product water quality and energy efficiency, *Membr. Sci.*, 568 (2018) 76–86.
- [19] T.A. Otitoju, R.A. Saari, A.L. Ahmad, Progress in the modification of reverse osmosis (RO) membranes for enhanced performance, *Ind. Eng. Chem.*, 67 (2018) 52–71.
- [20] T. Tsuru, S. Sasaki, T. Kamada, T. Shintani, T. Ohara, H. Nagasawa, K. Nishida, M. Kanezashi, T. Yoshioka, Multi-layered polyamide membranes by spray-assisted 2-step interfacial polymerization for increased performance of trimesoyl chloride (TMC)/m-phenylenediamine (MPD)-derived polyamide membranes, *J. Membr. Sci.*, 446 (2013) 504–512.
- [21] W. Xie, G.M. Geise, B.D. Freeman, H.S. Lee, G. Byun, J.E. McGrath, Polyamide interfacial composite membranes prepared from m-phenylene diamine, trimesoyl chloride and a new disulfonated diamine, *Membr. Sci.*, 403–404 (2012) 152–161.
- [22] A.H.M. El-Aassar, Polyamide thin film composite membranes using interfacial polymerization: synthesis, characterization and reverse osmosis performance for water desalination, *Basic Appl. Sci.*, 6 (2012) 382–391.
- [23] G. Kang, C. Gao, W. Chen, X. Jie, Y. Cao, Q. Yuan, Study on hypochlorite degradation of aromatic polyamide reverse osmosis membrane, *Membr. Sci.*, 300 (2007) 165–171.
- [24] M. Wilf, C. Bartels, Optimization of seawater RO systems design, *Desalination*, 173 (2005) 1–12.
- [25] C. Hobbs, S. Hong, J. Taylor, Effect of surface roughness on fouling of RO and NF membranes during filtration of a high organic surficial groundwater, *Water Supply Res. Technol.*, 55 (2006) 559–570.
- [26] E.M. Vrijenhoek, S. Hong, M. Elimelech, Influence of membrane surface properties on initial rate of colloidal fouling of reverse osmosis and nanofiltration membranes, *Membr. Sci.*, 188 (2001) 115–128.
- [27] C.J. Gabelich, J.C. Frankin, F.W. Geringer, K.P. Ishida, I.H. Suffet, Enhanced oxidation of polyamide membranes using monochloramine and ferrous iron, *Membr. Sci.*, 258 (2005) 64–70.